Readout circuit with improved sensitivity for contactless LC sensing tags

M. A. Carvajal, P. Escobedo, A. Martínez-Olmos, and A. J. Palma

***Abstract*— In this work we present a novel technique to estimate the resonance frequency of LC chipless tags (inductor-capacitor parallel circuit) with improved sensitivity and linearity. The developed reader measures the power consumption of a Colpitts oscillator during a frequency sweep. The readout circuit consists of a Colpitts oscillator with a coil antenna, varactor diodes to change the oscillator frequency, analog circuitry to measure the power consumption and a microcontroller to control the whole system and send the data to a PC via USB. When an LC tag is inductively coupled to the oscillator, without contact, a maximum power peak is found. As shown by an experimental calibration using an LC tag made on FR4 substrate, the frequency of this maximum is related to the resonance frequency. Both parameters, power consumption and resonance frequency, present an excellent linear dependence with a high correlation factor (R^2 = 0.995). Finally, a screen-printed LC tag has been fabricated and used as relative humidity sensor achieving a sensitivity of (-2.41 ± 0.21) kHz/% with an R^2 of 0.946.**

***Index Terms*—Contactless measurement, Readout system, Colpitts oscillator, Power measurement, LC tag.**

I. Introduction

Inductor-capacitor (LC) resonant circuits can be used for low-cost, simple, passive and wireless sensing purposes [1]. To that end, the impedance of an LC resonant circuit can be measured via inductive coupling between the sensor and the reader unit. Depending on the transduction principle, the capacitance, inductance or resistance of the LC sensing circuit is affected by the measurand, allowing both physical and chemical sensors. Therefore, various kinds of passive wireless LC sensors have been developed to measure parameters inside sealed or harsh environments [2]–[6], e.g., pressure inside the human body [7]–[9], electrocardiogram [8], high temperatures in internal combustion engines [10], quality of packaged food [11] [12], water content in building materials [13], pH control [14], temperature [6], [15], [16], and relative humidity [17]–[21], among others.

The LC sensor consists of a capacitor in parallel with an inductor, which forms an LC tank circuit with a variable resonance frequency modulated by the parameters to measure. The remote detection of this resonant frequency is based on the inductive coupling with an external readout system. Network or impedance analysers have been used as readout devices for resonance sensors [22]–[24]. Although adaptable and accurate, these instruments are bulky and expensive, thus their use outside the laboratory may be limited. Other options are phase locked loops [25] and devices measuring impedance as a function of frequency [7], [26].

To overcome these constraints, some authors have designed readout circuits for LC sensors to improve the accuracy and robustness of the overall system. Coosemans et al. designed a readout circuit based on a voltage-controlled oscillator (VCO), where the readout coil and a varactor constituted the frequency selection circuit of the VCO [27]. During the VCO sweep (20 – 40 MHz), the resonant frequency was detected as a voltage dip in the voltage across the reader coil. Alternatively, Pichorim and Abatti presented a measurement technique to avoid constraints with sweep time and/or transient components, where the LC sensor was excited using three simultaneous signals at different frequencies (around 300 kHz) [28]. The resonant frequency and quality factor (Q) were calculated from the three signals received by the reading coil. Jacquemod et al. proposed a reader architecture with low k-coupling factor compensation to improve the measurement distance, showing promising results up to 5 cm [29]. Their design was based on a self-oscillating loop improved by an anti-resonance cancellation network for low coupling factors (long distances between the LC sensor and the readout coil). The oscillating frequency shifted with respect to the resonant frequency of the LC sensor. Nopper et al. designed an analog frontend circuit based on coherent demodulation for mapping the real part of the reader coil impedance to a DC output voltage, thus minimizing the influence of the coupling factor [30], [31]. A digital signal-processing unit continuously readjusted the frequency of the excitation signal. Other readout circuits based on similar methods have been presented in the literature [25], [32], where the impedance change of the readout coil was obtained by combining the reference signal and the modulated signal, which was a function of the coil's impedance. Sardini et al. proposed a custom-made device that measures both the real and imaginary parts of the admittance

This work was supported by projects CTQ2016-78754-C2-1-R and FPA2015-67694-P from the Spanish Ministry of Economics and Competitivity and the European Regional Development Fund (ERDF).; and PI-0505-2017 within the biomedical and health sciences research, development and innovation projects in Andalucía. P. E. wants to thank the Spanish Ministry of Education, Culture and Sport for a pre-doctoral grant (FPU13/05032).

M. A. Carvajal, A. Martínez-Olmos and A. J. Palma are with the Department of Electronics and Computer Technology, ETSIIT C/Pta. Daniel Saucedo Aranda s/n, University of Granada, 18071 Granada, Spain. M. A. C. and A. J. P. are with Sport and Health Univ. Research Institute (iMUDS), University of Granada (e-mail: carvajal@ugr.es; pabloescobedo@ugr.es; amartinez@ugr.es; ajpalma@ugr.es). P. Escobedo is with Bendable Electronics and Sensing Technologies (BEST) Group, School of Engineering, University of Glasgow, G12 8QQ, Glasgow, UK. Corresponding author: M. A. Carvajal.

[33]. Their device included a digital synthesizer, three analog multipliers for downmixing the high frequency input, a microcontroller unit, and an analog-to-digital converter. Bao et al. presented a novel differential transduction circuit with improved sensitivity to the phase change (when the LC sensor coupled to the readout coil), thus enabling precise resonant frequency detection and further enlarging the sensing distance [34]. Therefore, despite the notable efforts in this field, further improvement is needed in the readout circuit design to achieve more reliable and precise results.

In a previous work, our research group proposed a low-cost handheld readout system for chipless passive LC tags, focusing the application of this technique on contactless relative humidity determination [20]. In that work, the sensing capacitance included in an LC tag was directly coupled to the coil of a Colpitts oscillator. Consequently, variations in the sensing capacitance produced changes in the oscillator frequency. The sensing capacitance was measured by registering the frequency oscillator shift. This frequency was monitored with the built-in logic counter of a low-cost microcontroller, resulting in a simple readout circuit. In the present work a different measurement strategy is proposed, which has required changes in the readout circuit while keeping it as simple as possible. In this work, changes in the maximum power consumption of the Colpitts oscillator due to changes in a coupled LC sensing tag have been accurately monitored by means of a frequency sweep. This technique has been validated by comparison with impedance analyser measurements, providing improved sensitivity than our previous design and linear response in the whole measurand range when applied to relative humidity determination. In the Experimental section, we describe the principle of detection and the hardware to implement it, along with the measurement procedure. The measurement system calibration and main specifications are shown in the Results and Discussion section, together with its application to relative humidity determination. In this section, we conduct a comparative study with our previous work. Finally, main conclusions are drawn.

II. Experimental

A. Materials and methods

Reader circuit was fabricated in our laboratory on FR4 printed circuit board (PCB) with a standard thick cooper (35 µm) using a milling machine model ProtoMat® S100 (LPKF Laser & Electronics AG, Garbsen, Germany). To calibrate the system, we fabricated an LC tag on FR4 substrate with a planar coil of 2.5 µH, a trimmer capacitor and a 4.7 kΩ resistor, both placed in parallel with the coil and a fixed capacitor. The variable capacitor was included to change the tag´s resonant frequency, while the parallel resistance simulates the effect of loss resistance of the tag coil to achieve a quality factor (Q) of 23. This targeted Q factor was similar to the LC sensing tag quality factor. For the application of relative humidity determination, the LC sensing tag was screen-printed using a Serfix III screen printing machine (Seglevint SL, Barcelona, Spain) on 75 µm thick flexible Polyimide Kapton® HN substrate (DuPont™, Wilmington, DE, USA). The screen mesh consisted of an aluminium rectangular structure of 50 cm × 35 cm with mesh density of 120 Nylon threads per centimetre (T/cm), which allowed a minimum width pattern of 300 µm. The patterns were screen-printed using the conductive silver-based ink SunTronic CRSN 2442 (Sun Chemical, New Jersey, USA). A thermal sintering process was carried out after printing at 120 °C during 20 minutes inside a convection air oven Venticell VC55 (MMM Medcenter Einrichtungen GmbH, Munich, Germany). Finally, a bridge line was attached to close the circuit using the conductive resin Epoxy EPO-TEK® H20E (Epoxy Technology Inc., Billerica, USA). The Epoxy resin was cured in the oven at 150 °C for 15 minutes. The design of the reader coil and the printed LC tag for humidity measurements was the same used in our previous work [20], which was optimized via numerical simulation using Advanced Design System (ADS) simulator (Keysight Technologies, Santa Clara, CA, USA) and COMSOL Multiphysics® (Comsol Inc., Burlington, MA, USA).

The precision impedance analyser Agilent 4294A (Agilent Technologies, Santa Clara, CA, USA) was used to measure the impedance from 10 to 20 MHz of the different circuit elements and coils. A climatic chamber VCL4006 (Vötsch Industryetedhnik, Balingen, Germany) held the experimental setup for the humidity measurements. Data processing for results extraction were conducted using Octave software.

B. Principle of measurement and global system architecture

The measurement technique is based on the fundamentals of a Colpitts oscillator. The active device of this type of oscillators can be a field-effect transistor or a bipolar transistor. We have selected a bipolar transistor (BJT) as in the oscillator configuration of our previous work [20]. Fig. 1 depicts the global system architecture, whose main blocks are: i) the Colpitts oscillator, ii) an analog conditioning stage, iii) the printed LC tag that will be used as the sensing element, iv) a microcontroller unit (MCU), and v) an external computer for digital signal processing and results display. All these elements will be explained in depth in the following subsection.

Regarding our proposed measurement technique, it is well

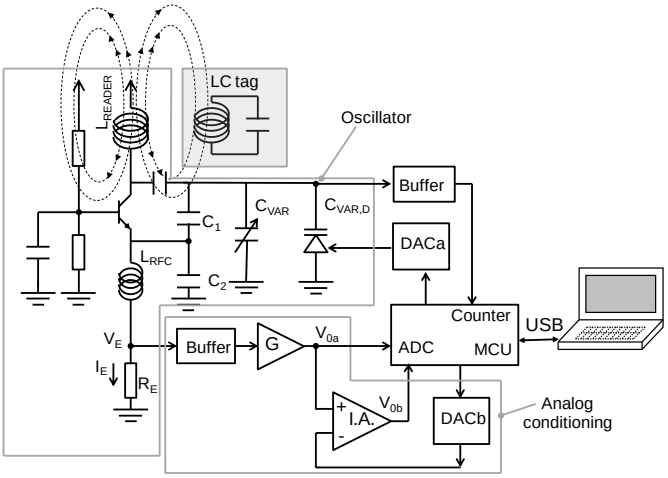

Fig. 1. Block diagram of the measurement system.

known that in a single-device transformer-coupled oscillator, the emitter current of the BJT (I_E) is related to the voltage amplitude of the fundamental harmonic (V_{oA}) in the load (R_L) as follows [35]:

$$V_{oA} \approx K_B \left(\alpha - \frac{1}{n}\right) R_L I_E \quad (1)$$

As seen in [35, eq. (11.35)], K_B is equal to $2I_1(d)/I_0(d)$, being $I_m(d)$ the modified Bessel function of order m, and d a parameter that is higher than 6 in the cases of magnitudes large in fundamental harmonic, like sinusoidal oscillators. In these cases, K_B varies from 1.8 to 1.95 approximately, as illustrated in [35, Fig. 11.5], being 1.9 a typical value. Continuing with eq. (1), $\alpha = (1+\beta)/\beta$, being β the current gain of the transistor (I_C/I_B); and n is the turns ratio (N_1/N_2) between the primary winding (the oscillator coil) and the secondary winding (load coil), assuming an ideal magnetic coupling (k=1). Therefore, the power consumption of the oscillator is approximated as the product of the emitter current and the power supply voltage, 5 V in our case. Consequently, the power consumption of the oscillator is proportional to the voltage output.

As shown in Fig. 1, the oscillator resistive load consists of the parallel equivalent series resistors of the reader and the tag coils. Indeed, the load is not directly connected to the oscillator output of our system, but it sources from the inductive coupling between the reader coil and the LC tag. Moreover, the effective load resistance of the coupled LC tag depends on the relationship between the resonant frequency of the tag and the oscillator frequency. The LC tag is characterized by its resonant frequency and its equivalent parallel resistance, which is mainly due to the parasitic resistance of the tag coil. Once the LC tag is coupled to the oscillator, a decrease of the oscillator frequency is produced due to the tag capacitance, as it was shown in our previous work [20]. In this situation, if we perform an oscillator frequency sweep in the Colpitts oscillator around the already decreased frequency, a maximum of the power delivered to the load will be found when the oscillator frequency is coupled in resonance with the LC tag. This is the principle of the proposed measurement technique that, to the best of our knowledge, has not been implemented before in the context of sensing applications.

In the proposed system, the frequency sweep is performed by means of the capacitance variation through the variable capacitor and the varactor diode in the circuit design (see C_{VAR} and $C_{VAR,D}$ in Fig. 1). On the other hand, to measure the power delivered by the oscillator during the capacitance variation (and, consequently, during the frequency sweep), the emitter current, I_E, is monitored. I_E is approximately equal to the collector current if the BJT current gain, β, is much higher than the unity at the oscillation frequency (usual at low frequencies). Therefore, a maximum of the emitter current will take place when the LC tag and the oscillator are in resonance. Changes in the height of the maximum of the emitter current (I_E) will thus indicate changes in the resistance load. Changes in the value of the frequency of this maximum will indicate that the resonance frequency of the LC tag has shifted. In this work, this latter variation of the delivered power peak will be used as measurement parameter when the LC tag resonant characteristics change because of an environmental (physical or chemical) magnitude. In particular, we will show that relative humidity changes in the surrounding atmosphere of the LC tag can be accurately detected with this contactless technique, which could be applied to the monitoring of modified atmosphere packages (MAP).

C. Readout circuit architecture

Fig. 2 depicts the functional block structure of the developed hardware. As previously mentioned, the reader unit is based on a Colpitts oscillator, a module to accurately measure the power consumption of the oscillator, and a microcontroller unit (MCU). The oscillator is based on the bipolar transistor model 2N2369 (NXP Semiconductors, Eindhoven, Netherlands). This transistor has a transition frequency of 500 MHz and maximum power consumption of 360 mW, which are suitable parameters for our application. The frequency oscillation can be tuned using the trimmer C_{VAR}. Once the frequency oscillation is set to the frequency range of interest (around 13 MHz), a fine sweep is conducted by biasing the varactor diode, C_D, at different voltages using the digital to analog converter. The oscillation frequency without tag is given by [36]:

$$f_{osc} = \frac{1}{2\pi}\sqrt{\frac{1}{L_{READER}(C_S+C_D+C_{VAR})}}, \quad (2)$$

where $C_S^{-1} = C_1^{-1} + C_2^{-1}$. L_{READER} is a PCB coil (see Fig. 2) with three loops of 8x8 cm^2, being L_{osc}= 2.546 ± 0.004 µH at 13.56 MHz with a quality factor of Q = 60.2±0.9, similar to the coil used in our previous work [20]. The measured self-resonance frequency was 38.93±0.17 MHz. Two identical ceramic capacitors of 22 pF were used as C_1 and C_2. The varactor diode in this application was a low-voltage operation device model BB202.115 (NXP Semiconductor, Eindhoven,

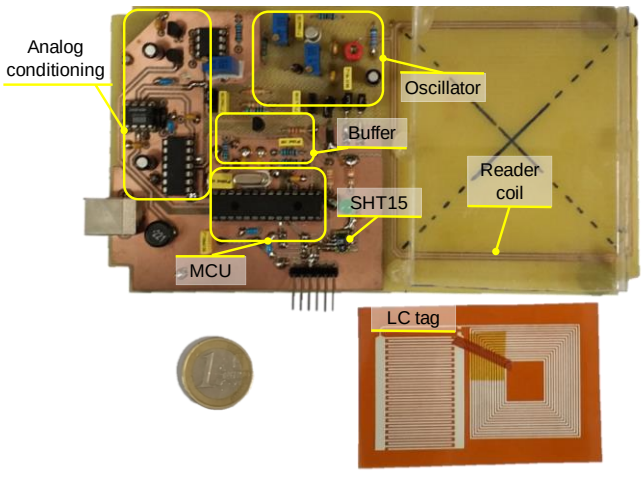

Fig. 2. Photographs of the measurement system showing the relevant components: (top) the readout circuit, and (bottom) the printed LC tag for humidity sensing applications.

This article has been accepted for publication in a future issue of this journal, but has not been fully edited. Content may change prior to final publication. Citation information: DOI 10.1109/JSEN.2019.2943002, IEEE Sensors Journal

Netherlands). The emitter resistor, R_E, had a value of 270 Ω to achieve a collector current of 1.6 mA.

During the fine capacitance sweep, the voltage in R_E, V_E, is amplified in a non-inverting amplifier with 5.7 V/V gain. For this purpose, the LT1366 (Analog Devices, Norwood, MA, USA) was selected due to its rail-to-rail input-output operation and high input impedance to avoid current losses. The microcontroller then digitalizes its output, V_{0a}.To increase the measurement resolution, another amplification stage based on an instrumentation amplifier (IA) is included as shown in Fig. 1, which allows an initial zeroing step. To do that, the V_{0a} output is connected to the non-inverting input, while channel B of the digital to analog converter (DAC) is connected to the IA inverting input to carry out the zeroing, as it will be explained below. The selected DAC was the MPC4922 (Microchip, Chandler, AZ, USA). The instrumentation amplifier INA114 (Texas Instruments, Dallas, TX, USA) was configured to provide a differential voltage gain of 6 V/V, thus achieving a total gain of 34.2 V/V.

A PIC18F2553 microcontroller (Microchip, Chandler, AZ, USA) controls the whole measurement process. This model was selected due to its 12-bit analog-to-digital converter, USB communication capability, timer and counter modules. The buffered oscillator output is connected to the MCU counter input (see Fig. 1), and the pulses are measured during two overflow periods of 25 ms of the MCU timer. Therefore, the frequency measurement elapses in 50 ms.

D. Measurement procedure

To improve the measurement resolution, we implemented an algorithm of zeroing using the DAC. This method involves two frequency sweeps: the first one to set the zero of the system, and the second one to measure the amplified emitter voltage, V_E, which is proportional to the power consumption. Therefore, the measurement procedure is initialized with a frequency sweep to determine the maximum and minimum oscillator power consumption, measuring the V_{0a} voltage (without amplification by the IA, see Fig. 1). The frequency sweep is conducted by biasing the varactor diode with the DAC (channel A) at different voltages. Then, the output B of the DAC is set to the minimum measured V_{0a} voltage and connected to the IA inverting input in order to reduce the IA output to 200 mV. With this configuration, a second frequency sweep is carried out, measuring the oscillator frequency and the V_{0a} and V_{0b} voltages (see Fig. 1). The V_{0b} voltage is not only amplified, but also low-pass filtered because of the limited IA bandwidth-gain product. In the case of the INA114, the gain-bandwidth product is equal to 1 MHz. The gain is set at 6 V/V (using a 10 kΩ precision resistor), obtaining a bandwidth of 167 kHz, which is much lower than the oscillator frequency (above 10 MHz). Finally, the power consumption, P, as a function of the frequency is calculated multiplying the measured V_E voltage by the emitter resistor R_E (see Fig. 1).

To check the reliability of this procedure, we have digitally processed both the amplified voltage V_{0b} and the direct voltage V_{0a} by averaging ten consecutive samples. After that, we fitted the four curves (with/without amplification and with/without averaging) to a Gaussian function in the computer. As previously mentioned, bandwidth limitation of the instrumentation amplifier provides enough low-pass filtering to the amplified signal, V_{0b}, as shown in Fig. 3.

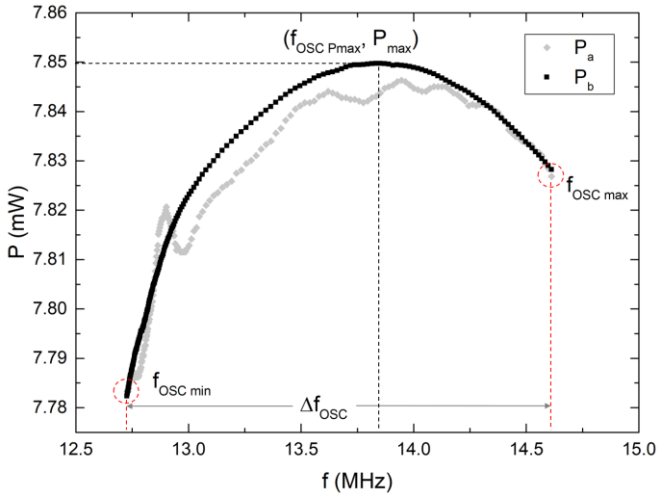

Fig. 3. Experimental digital filtered results of current conversion (V_{0a}, in grey) and amplified current conversion (V_{0b}, in black). The experimental data were obtained with a 40% relative humidity atmosphere using the LC sensing tag. The initial (f_{OSC_MIN}) and final point (f_{OSC_MAX}) of the frequency sweep (Δf_{OSC}) are highlighted in the figure for better comprehension.

III. Results and Discussion

In this section, we describe the calibration of the system and its application for environmental relative humidity determination.

A. Reader calibration and specifications

Firstly, we conducted a frequency sweep without any coupled LC tag in order to evaluate the frequency reduction once the tag is coupled. Without LC tag, the frequency oscillator ranged from 12.8 to 14.3 MHz. When the printed LC sensing tag was inductively coupled, the oscillator frequency varied from 11.7 to 12.8 MHz. As it was expected, a significant oscillator frequency reduction was found.

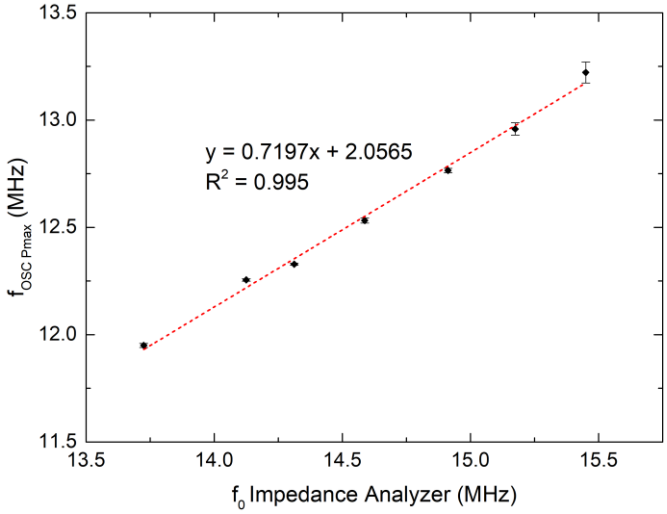

Fig. 4. Correlation between the resonant frequency, f_o, measured by the Impedance Analyser and the results obtained with our measurement system.

This article has been accepted for publication in a future issue of this journal, but has not been fully edited. Content may change prior to final publication. Citation information: DOI 10.1109/JSEN.2019.2943002, IEEE Sensors Journal

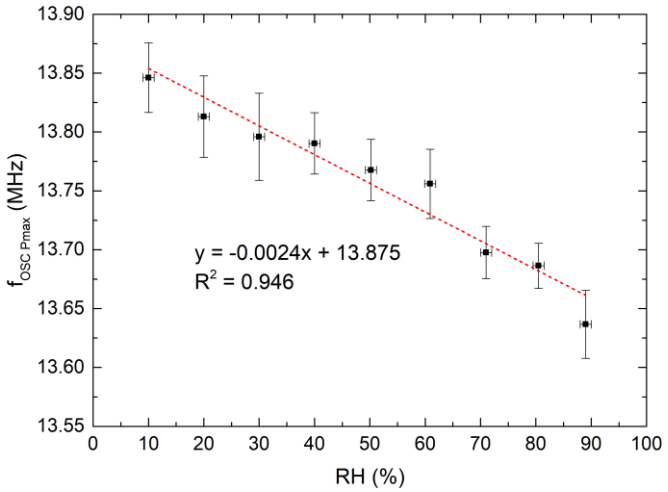

Fig. 5. Frequency at maximum power consumption as function of the relative humidity.

For calibration purposes, the LC tag fabricated on FR4 was placed over the reader coil (with an air gap of 1 cm between coils) and a frequency oscillation sweep was automatically conducted by the reader changing the reverse bias of the variable capacitance diode, as described above. The reader provided the emitter current as a function of the frequency. According to the described procedure, a software calculated the frequency of the maximum power point, f_{osc_Pmax}. Simultaneously, the resonance frequency, f_o, was measured with the Impedance Analyser. Fig. 4 depicts the correlation between both data. Our experimental results corresponding to the amplified and filtered data are shown with dots and their corresponding error bars (standard deviation), while the dashed line represents the linear fitting. Using this calibration curve, the resonant frequency of the LC sensing tag can be calculated.

B. Application: relative humidity monitoring

We have applied our measurement system for environmental relative humidity (RH) monitoring. To that end, screen printed LC tags were designed and fabricated as in our previous work [20], see Fig. 2. The tag capacitance increases with humidity due to the increment of the electrical permittivity of the underlying Kapton substrate because of the water absorption [37], [38]. This capacitance increase produces a reduction of the tag resonant frequency. Keeping in mind the correlation shown in Fig. 4, the frequency at the maximum power peak will also decrease.

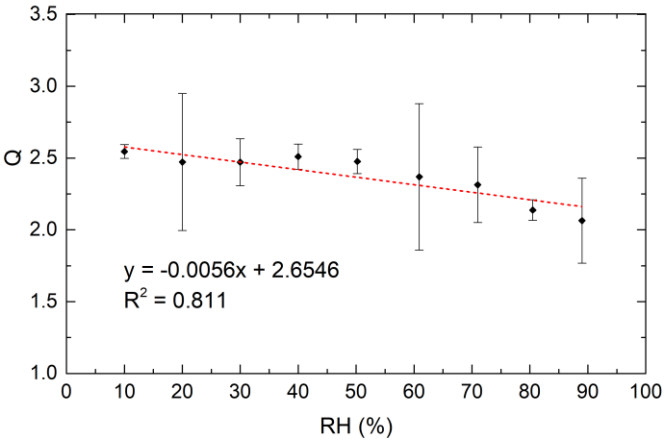

Fig. 6. Global quality factor of the whole system as a function of the relative humidity.

A set of five individual planar inductors and capacitors were fabricated and electrically characterized. The average measured value for the inductors was 7.88 ± 0.09 µH at 13.56 MHz with an average quality factor of 2.11 ± 0.12. As for the capacitors, an average capacity value of 18.6 ± 0.4 pF was measured at the same frequency. To conduct the experiments, we fixed and centered the printed LC tag over the reader coil at a distance of 1 cm in the vertical axis. Then, we placed the whole system into the climatic chamber. The stationary humidity conditions of the LC tag were controlled inside the climatic chamber at constant temperature (20 ºC). Three set of measurements were taken for each relative humidity value to obtain a representative average value. Humidity inside the climate chamber was measured using the SHT15 sensor (Sensirion AG, Staefa, Switzerland) included in the readout unit, which has a typical accuracy of ±2.0% RH. We varied relative humidity from 10% up to 90% and the frequency of the maximum power of the oscillator was calculated with a significant change of 220 kHz in that RH range. Fig. 5 shows the rather linear dependence obtained between the frequency at maximum power and the RH with a slope of (-2.41 ± 0.21) kHz/%. The dependence of the quality factor of the whole system (Q) with RH was also studied. Q was calculated as the ratio between the $f_{oscPmax}$ and the bandwidth (BW), Q = $f_{oscPmax}$/BW. The BW was computed from the sigma parameter of the Gaussian fit curve by extrapolating the point of half-maximum power. Fig. 6 shows the obtained results, where a degradation of the quality factor with relative humidity can be observed, being more significant at high HR values. The high uncertainty obtained due to the extrapolation makes this parameter unsuitable for relative humidity measurements.

To evaluate the response using our previous technique [20], the minimum oscillator frequency (f_{OSC_MIN}, see Fig. 3) was also obtained from each power-frequency curve at different relative humidity values. To compare the present and previous

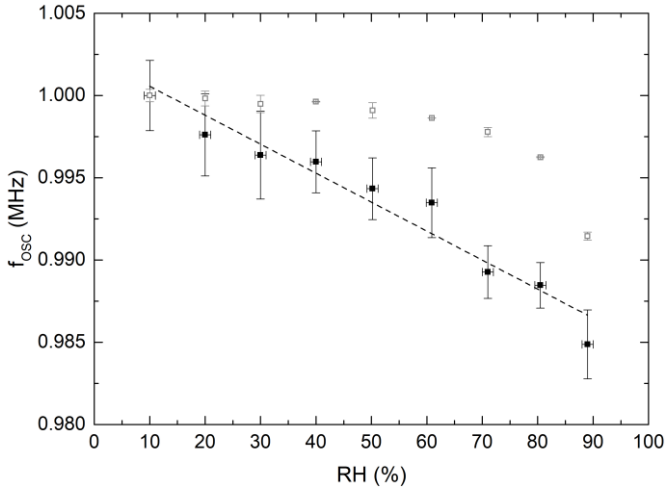

Fig. 7. Comparison between the resonance frequency obtained with our previous technique (empty symbols) and the frequency at maximum power consumption from this work (solid symbols), showing the linearity and sensitivity improvements.

method, the results normalized to 10% RH are displayed as a function of the relative humidity (Fig. 7). Empty symbols represent the results obtained with our previous technique, while solid symbols are the ones obtained with the new technique. Error bars are the result of standard deviations. A better linear trend can be observed in the results derived from this work, providing greater sensitivity in the whole RH range. Therefore, the proposed measurement technique can be considered as a significant improvement in the field of LC-based contactless sensing.

IV. Conclusion

In this work, we have described and experimentally validated a novel contactless technique to measure the resonant frequency of LC tags. The proposed technique is based on a simple circuit topology: a Colpitts oscillator, a frequency-meter and analog circuitry to measure the power consumption. Therefore, this novel approach can be deployed to measure capacitive sensors in a contactless way. The readout circuit implementing the proposed measurement procedure has been validated through an example of application to measure environmental humidity, achieving improved sensitivity, (-2.41 ± 0.21) kHz/%, and linearity ($R^2 = 0.945$) with respect to our previous work [20]. Linearity can be further enhanced if the sensor presents a linear behaviour, as it can be concluded from the calibration process, where a high correlation factor was found ($R^2 = 0.995$). The proposed technique can be used for capacitive sensors by measuring the shift of the maximum power frequency, as reported in the present work. In addition, changes in the height of this maximum are related to changes in the quality factor of the LC sensor tag. Therefore, the application of this method to resistive sensors could be a future line of work. The measurement technique here presented and validated can be suitable for contactless measurements in the context of smart packaging or artwork conservation, among other applications.

References

[1] Q.-A. Huang, L. Dong, and L.-F. Wang, "LC Passive Wireless Sensors Toward a Wireless Sensing Platform: Status, Prospects, and Challenges," *J. Microelectromechanical Syst.*, vol. 25, no. 5, pp. 822–841, Oct. 2016.

[2] C. Li *et al.*, "Review of Research Status and Development Trends of Wireless Passive LC Resonant Sensors for Harsh Environments," *Sensors*, vol. 15, no. 6, pp. 13097–13109, Jun. 2015.

[3] K. G. Ong and C. A. Grimes, "A resonant printed-circuit sensor for remote query monitoring of environmental parameters," *Smart Mater. Struct.*, vol. 9, no. 4, pp. 421–428, Aug. 2000.

[4] K. G. Ong, C. A. Grimes, C. L. Robbins, and R. S. Singh, "Design and application of a wireless, passive, resonant-circuit environmental monitoring sensor," *Sensors Actuators A Phys.*, vol. 93, no. 1, pp. 33–43, Aug. 2001.

[5] J. B. Ong, Z. You, J. Mills-Beale, E. L. Tan, B. D. Pereles, and K. G. Ong, "A Wireless, Passive Embedded Sensor for Real-Time Monitoring of Water Content in Civil Engineering Materials," *IEEE Sens. J.*, vol. 8, no. 12, pp. 2053–2058, Dec. 2008.

[6] Y. Wang, Y. Jia, Q. Chen, and Y. Wang, "A Passive Wireless Temperature Sensor for Harsh Environment Applications," *Sensors*, vol. 8, no. 12, pp. 7982–7995, Dec. 2008.

[7] C. C. Collins, "Miniature Passive Pressure Transensor for Implanting in the Eye," *IEEE Trans. Biomed. Eng.*, vol. BME-14, no. 2, pp. 74–83, Apr. 1967.

[8] P.-J. Chen, S. Saati, R. Varma, M. S. Humayun, and Y.-C. Tai, "Wireless Intraocular Pressure Sensing Using Microfabricated Minimally Invasive Flexible-Coiled LC Sensor Implant," *J. Microelectromechanical Syst.*, vol. 19, no. 4, pp. 721–734, Aug. 2010.

[9] G.-Z. Chen, I.-S. Chan, and D. C. C. Lam, "Capacitive contact lens sensor for continuous non-invasive intraocular pressure monitoring," *Sensors Actuators A Phys.*, vol. 203, pp. 112–118, Dec. 2013.

[10] M. A. Fonseca, J. M. English, M. von Arx, and M. G. Allen, "Wireless micromachined ceramic pressure sensor for high-temperature applications," *J. Microelectromechanical Syst.*, vol. 11, no. 4, pp. 337–343, Aug. 2002.

[11] Y. Feng, L. Xie, Q. Chen, and L.-R. Zheng, "Low-Cost Printed Chipless RFID Humidity Sensor Tag for Intelligent Packaging," *IEEE Sens. J.*, vol. 15, no. 6, pp. 3201–3208, Jun. 2015.

[12] E. Tan, W. Ng, R. Shao, B. Pereles, and K. Ong, "A Wireless, Passive Sensor for Quantifying Packaged Food Quality," *Sensors*, vol. 7, no. 9, pp. 1747–1756, Sep. 2007.

[13] G. Stojanović, M. Radovanović, M. Malešev, and V. Radonjanin, "Monitoring of Water Content in Building Materials Using a Wireless Passive Sensor," *Sensors*, vol. 10, no. 5, pp. 4270–4280, Apr. 2010.

[14] S. Bhadra, D. J. Thomson, and G. E. Bridges, "Monitoring acidic and basic volatile concentration using a pH-electrode based wireless passive sensor," *Sensors Actuators B Chem.*, vol. 209, pp. 803–810, Mar. 2015.

[15] C. Li, Q.-L. Tan, C.-Y. Xue, W.-D. Zhang, Y.-Z. Li, and J.-J. Xiong, "Wireless contactless pressure measurement of an LC passive pressure sensor with a novel antenna for high-temperature applications," *Chinese Phys. B*, vol. 24, no. 4, p. 048801, Apr. 2015.

[16] Q. Tan *et al.*, "Wireless Passive Temperature Sensor Realized on Multilayer HTCC Tapes for Harsh Environment," *J. Sensors*, vol. 2015, pp. 1–8, Oct. 2015.

[17] J. Fernandez-Salmeron, A. Rivadeneyra, M. A. C. Rodriguez, L. F. Capitan-Vallvey, and A. J. Palma, "HF RFID Tag as Humidity Sensor: Two Different Approaches," *IEEE Sens. J.*, vol. 15, no. 10, pp. 5726–5733, Oct. 2015.

[18] E. M. Amin, M. S. Bhuiyan, N. C. Karmakar, and B. Winther-Jensen, "Development of a Low Cost Printable Chipless RFID Humidity Sensor," *IEEE Sens. J.*, vol. 14, no. 1, pp. 140–149, Jan. 2014.

[19] J. Salmerón, A. Albrecht, S. Kaffah, M. Becherer, P. Lugli, and A. Rivadeneyra, "Wireless Chipless System for Humidity Sensing," *Sensors*, vol. 18, no. 7, p. 2275, Jul. 2018.

[20] P. Escobedo *et al.*, "Compact readout system for chipless passive LC tags and its application for humidity monitoring," *Sensors Actuators A Phys.*, vol. 280, pp. 287–294, Sep. 2018.

[21] M.-Z. Xie, L.-F. Wang, L. Dong, W.-J. Deng, and Q.-A. Huang, "Low Cost Paper-Based LC Wireless Humidity Sensors and Distance-Insensitive Readout System," *IEEE Sens. J.*, vol. 19, no. 12, pp. 4717–4725, Jun. 2019.

[22] D. Marioli, E. Sardini, M. Serpelloni, and A. Taroni, "A new measurement method for capacitance transducers in a distance compensated telemetric sensor system," *Meas. Sci. Technol.*, vol. 16, no. 8, pp. 1593–1599, Aug. 2005.

[23] V. Sridhar and K. Takahata, "A hydrogel-based passive wireless sensor using a flex-circuit inductive transducer," *Sensors Actuators A Phys.*, vol. 155, no. 1, pp. 58–65, Oct. 2009.

[24] R. A. Potyrailo, N. Nagraj, Z. Tang, F. J. Mondello, C. Surman, and W. Morris, "Battery-free Radio Frequency Identification (RFID) Sensors for Food Quality and Safety," *J. Agric. Food Chem.*, vol. 60, no. 35, pp. 8535–8543, Sep. 2012.

[25] J. Riistama, E. Aittokallio, J. Verho, and J. Lekkala, "Totally passive wireless biopotential measurement sensor by utilizing inductively coupled resonance circuits," *Sensors Actuators A Phys.*, vol. 157, no. 2, pp. 313–321, Feb. 2010.

[26] Sajeeda and T. J. Kaiser, "Passive Telemetric Readout System," *IEEE Sens. J.*, vol. 6, no. 5, pp. 1340–1345, Oct. 2006.

[27] J. Coosemans, M. Catrysse, and R. Puers, "A readout circuit for an intra-ocular pressure sensor," *Sensors Actuators A Phys.*, vol. 110, no. 1–3, pp. 432–438, Feb. 2004.

[28] S. F. Pichorim and P. J. Abatti, "A novel method to read remotely resonant passive sensors in biotelemetric systems," *IEEE Sens. J.*, vol. 8, no. 1, pp. 3–7, 2008.

[29] G. Jacquemod, M. Nowak, E. Colinet, N. Delorme, and F. Conseil,

"Novel architecture and algorithm for remote interrogation of battery-free sensors," *Sensors Actuators, A Phys.*, vol. 160, no. 1–2, pp. 125–131, 2010.

[30] R. Nopper, R. Niekrawietz, and L. Reindl, "Wireless Readout of Passive *LC* Sensors," *IEEE Trans. Instrum. Meas.*, vol. 59, no. 9, pp. 2450–2457, Sep. 2010.

[31] R. Nopper, R. Has, and L. Reindl, "A wireless sensor readout system-circuit concept, simulation, and accuracy," *IEEE Trans. Instrum. Meas.*, vol. 60, no. 8, pp. 2976–2983, 2011.

[32] T. Salpavaara, J. Verho, P. Kumpulainen, and J. Lekkala, "Readout methods for an inductively coupled resonance sensor used in pressure garment application," *Sensors Actuators, A Phys.*, vol. 172, no. 1, pp. 109–116, 2011.

[33] E. Sardini and M. Serpelloni, "Wireless Measurement Electronics for Passive Temperature Sensor," *IEEE Trans. Instrum. Meas.*, vol. 61, no. 9, pp. 2354–2361, Sep. 2012.

[34] K. Bao *et al.*, "A readout circuit for wireless passive LC sensors and its application for gastrointestinal monitoring," *Meas. Sci. Technol.*, vol. 25, no. 8, p. 085104, Aug. 2014.

[35] D. O. Pederson and K. Mayaram, *Analog Integrated Circuits for Communication. Principles, Simulation and Design*, Second. Springer, 2011.

[36] H. L. Krauss, C. W. Bostian, and F. H. Raab, *Solid State Radio Engineering*. Canada: John Wiley & Sons, Inc., 1980.

[37] DuPont, "DUPONT™ KAPTON® Summary of properties," 2017. .

[38] T. Unander and H.-E. Nilsson, "Characterization of Printed Moisture Sensors in Packaging Surveillance Applications," *IEEE Sens. J.*, vol. 9, no. 8, pp. 922–928, Aug. 2009.